Synthesis of Water Soluble Graphene

Yongchao Si and Edward T. Samulski*

*Department of Chemistry, University of North Carolina at Chapel Hill,
Chapel Hill, North Carolina 27599*

ABSTRACT

A facile and scalable preparation of aqueous solutions of isolated, sparingly sulfonated graphene is reported. ^{13}C NMR and FTIR spectra indicate that the bulk of the oxygen-containing functional groups was removed from graphene oxide. The electrical conductivity of thin evaporated films of graphene (1250 S/m) relative to similarly prepared graphite (6120 S/m) implies that an extended conjugated sp[2] network is restored in the water soluble graphene.

Recently characterized as "the thinnest material in our universe",[1] graphene, a single-atom-thick sheet of hexagonally arrayed sp[2]-bonded carbon atoms, promises a diverse range of applications from composite materials to quantum dots.[2–7] However, just as with other newly discovered allotropes of carbon (fullerenes and single-wall nanotubes), material availability and processability will be the rate-limiting steps in the evaluation of putative applications of graphene. For graphene, that availability is encumbered by having to surmount the high cohesive van der Waals energy (5.9 kJ mol^{-1} carbon)[8] adhering graphitic sheets to one another. Herein, we describe a facile and scalable preparation of aqueous solutions of isolated, sparingly sulfonated graphene sheets starting from oxidized graphite. The measured electrical conductivity of contiguous films of graphene prepared by evaporation of an aqueous solution implies that the extensive conjugated sp[2] carbon network is restored in the water soluble graphene.

Graphene was initially isolated by mechanical exfoliation, peeling off the top surface of small mesas of pyrolytic graphite,[2,5] a method which is not suitable for large-scale application. More recently, single sheets of graphene oxide were chemically reduced to graphene after deposition on a silicon substrate,[9,10] again a method that lends itself to limited applications. Exfoliation of graphite oxidized with strong acids either by rapid thermal expansion[11] or by ultrasonic dispersion[12,13] is one approach to obtain (functionalized) graphene oxide in bulk. The oxidation chemistry is similar to that used to functionalize single-wall carbon nanotubes (SWNTs)[14–16] and yields a variety of oxygen functionalities (−OH, −O−, and −COOH) primarily at "defect" sites on SWNT ends. For sufficiently strong oxidizing agents, functionalized defects were also created on the SWNT wall surfaces.[17] Therefore, independent of the exfoliation mechan-

ics, graphene oxide prepared from oxidized graphite includes significant oxygen functionality[11] and defects so the associated structural and electronic perturbations caused by oxidation must be repaired to recover the unique properties of graphene. These perturbations can be superficially ameliorated with "passivation chemistry," for example, reacting graphene oxide with amines,[12] but the resulting materials are not expected to exhibit the electronic attributes of graphene because of residual (passivated) defects.

Ideally graphene oxide must be rigorously reduced after exfoliation to recover the desirable properties of graphene. To that end, polymer-coated "graphitic nanoplatelets" were obtained by reducing exfoliated graphite oxide in the presence of poly(sodium-4 styrene sulfonate) giving intriguing composite materials.[6,13] However, the presence of the polymeric dispersing agent in graphene composite may be undesirable for some applications. Reduction of exfoliated graphite oxide in the presence of ammonia can lead to the graphene nanosheets with limited water solubility (<0.5 mg/mL).[18] We report a chemical route to aqueous solutions of isolated graphene sheets by reducing graphene oxide in two stages. Our methodology removes residual oxygen functionality and introduces sulfonic acid groups in partially reduced graphene oxide in a controlled way. The charged −SO$_3^-$ units prevent the graphitic sheets from aggregating in solution after the final reduction stage of the graphene oxide thereby yielding isolated sheets of lightly sulfonated graphene with improved water solubility.

We use graphite oxide prepared by oxidizing graphite flakes with acid[19] as the starting material for the preparation of graphene. Like graphite, the oxidation product has a layered morphology with −OH and >O functionality disrupting the hexagonal carbon basal planes on the interior of multilayered stacks of graphene oxide; −COOH and carbonyl groups decorate the periphery of the planes. Correspondingly, graphite oxide exhibits an increased inter-

---

* Corresponding author. E-mail: et@unc.edu. Telephone: (919) 962-1561. Fax: (919) 962-2388.

layer spacing (from 0.34 nm in graphite to >0.6 nm in graphite oxide)[20] thereby weakening the van der Waals forces between layers and enabling facile exfoliation via sonication. The resulting highly functionalized graphene oxide forms stable dispersions in water. However, if the oxygen functionality is removed to yield graphene, the graphene sheets lose their water dispersability, aggregate, and eventually precipitate. In order to overcome this, we judiciously introduce a small number of p-phenyl-SO_3H groups into the graphene oxide before it is fully reduced and the resulting graphene remains soluble in water and does not aggregate.

We prepare graphene from graphene oxide in three steps: (1) prereduction of graphene oxide with sodium borohydride at 80 °C for 1 h to remove the majority of the oxygen functionality; (2) sulfonation with the aryl diazonium salt of sulfanilic acid in an ice bath for 2 h; and (3) postreduction with hydrazine (100 °C for 24 h) to remove any remaining oxygen functionality. The lightly sulfonated graphene can be readily dispersed in water at reasonable concentrations (2 mg/mL) in the pH range of 3−10. Isolated graphene sheets persist in the mixture of water and organic solvents including methanol, acetone, acetonitrile, thus making it possible to further modify its surface for applications such as reinforcements in composites. The sulfonation level is stoichiometrically controlled to enable water solubility with minimal impact on the unique properties of graphene. Prereduction (step 1) is necessary both to achieve complete reduction (in step 3) and to enable the sulfonation reaction (step 2) by increasing the size of sp^2-carbon domains for reaction with the aryl diazonium salt. For example, elemental analysis shows that after prereduction of graphene oxide one can, via the diazonium salt reaction, achieve a S:C ratio of 1:35, whereas only a 1:148 ratio is possible using unreduced graphene oxide under the same reaction conditions. After sulfonation, the addition of more sodium borohydride (in step 3) immediately precipitates graphitic carbon. However, when hydrazine was used in the final reduction step, there was no sign of precipitation even after reacting for 48 h at 100 °C. Elemental analysis confirms the presence of nitrogen in graphene with a N:C ratio of 1:31. The lightly sulfonated graphene remains as single carbon sheets in water after the sulfonated graphene oxide is reacted with hydrazine for 24 h. In contrast, the reduction of graphene oxide with hydrazine under the similar conditions leads to irreversible aggregation and precipitation of graphitic sheets in water.[13,18] This confirms the presence of negatively charged $-SO_3^-$ units which in turn, impart sufficient electrostatic repulsion to keep carbon sheets separated during reduction.

We have measured the zeta potentials of our aqueous dispersions of graphene and graphene oxide in an effort to corroborate Li et al.'s[18] rationale for the stability of such dispersions, that is, electrostatic stabilization of graphene sheets. Similar to graphene oxide, the lightly sulfonated graphene is also negatively charged. We find negative zeta potentials of 55−60 mV for our graphene (pH = 6, prepared by thoroughly rinsing with water until the pH is close to neutral); for graphene oxide, we find 60−70 mV (negative). These ranges of zeta potentials are ideal for stabilizing
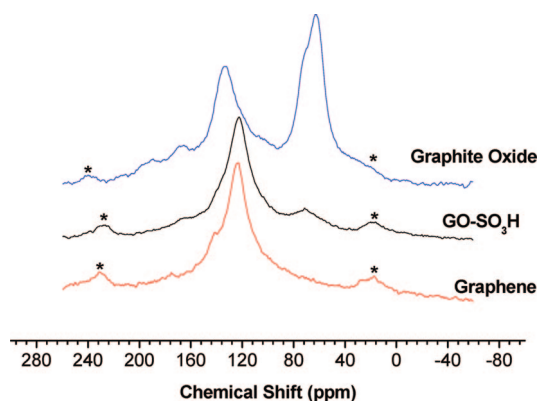

Figure 1. Solid state ^{13}C MAS NMR spectra (90.56 MHz; 9.4k rpm) of graphite oxide, sulfonated graphene oxide (GO-SO_3H) and graphene; *indicates spinning side bands.
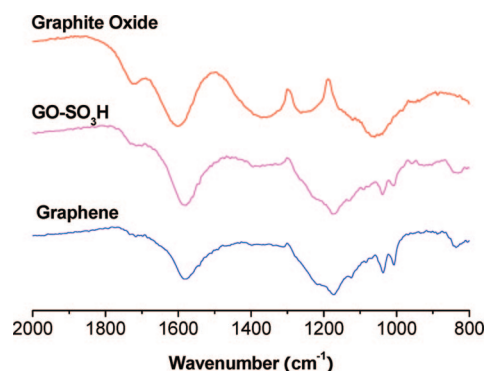

Figure 2. ATR-FTIR spectra of graphite oxide, sulfonated graphene oxide (GO-SO_3H) and graphene.

conventional colloidal particles;[21] ASTM defines colloids with zeta potentials higher than 40 mV (negative or positive) to have "good stability." Our aqueous dispersion of graphene show good stability: There is no sign of coagulation of graphene sheets after more than one month.

Solid state ^{13}C MAS NMR reflects the extent of graphene oxide reduction. Figure 1 shows ^{13}C NMR spectra of graphite oxide, sulfonated graphene oxide (GO-SO_3H) and graphene, respectively. Two distinct resonances dominate the spectrum of graphite oxide: The resonance centered at 134 ppm corresponds to unoxidized sp^2 carbons; the 60 ppm resonance is a result of epoxidation, and the 70 ppm shoulder is from hydroxylated carbons.[20,22,23] For graphite oxide with a low degree of oxidation, the latter resonances overlap, and a weak broad resonance corresponding to carbonyl carbons is observed at 167 ppm. After prereduction, the 60 ppm peak disappears, and the 70 ppm and 167 ppm resonances weaken significantly. The peak at 134 ppm shifts to 123 ppm because of the change in the chemical environment of the sp^2 carbons.[23] After the final reduction step to yield lightly sulfonated graphene, the resonances at 70 ppm and 167 ppm disappear; the small peak emerging at 140 ppm is attributed to carbons in the covalently attached phenyl-SO_3H groups; the resonance is not so obvious in the GO-SO_3H spectrum.

The NMR results are corroborated by attenuated total reflectance (ATR) FTIR spectra. The spectrum of graphite oxide illustrates the presence of C—O (ν_{C-O} at 1060 cm^{-1}),
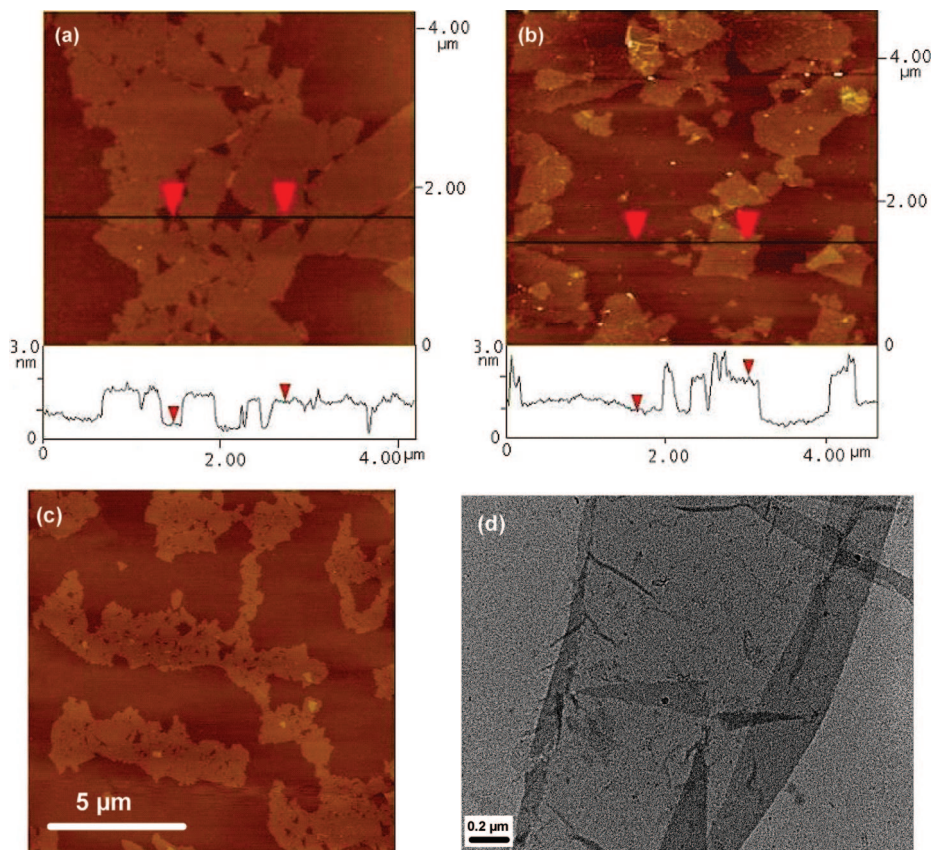
Figure 3. Images of isolated graphene oxide and graphene sheets. (a) AFM image of graphene oxide sheets on freshly cleaved mica, the height difference between two arrows is 1nm, indicating a single graphene oxide sheet; (b) AFM image of water-soluble graphene on freshly cleaved mica; the height difference between two arrows is 1.2 nm; (c) AFM image of large graphene oxide sheets on mica, small holes in the sheets are caused by overexposure to sonicaion; (d) TEM image of a partially folded water-soluble graphene sheet.

C—O—C (ν_{C-O-C} at 1250 cm^{-1}), C—OH (ν_{C-OH} at 1365 cm^{-1}), and C=O in carboxylic acid and carbonyl moieties ($\nu_{C=O}$ at 1720 cm^{-1}).[20,22,24,25] The peak at 1600 cm^{-1} may be from skeletal vibrations of unoxidized graphitic domains,[25] domains apparent in the ^{13}C NMR spectrum of graphite oxide. After prereduction and sulfonation, the peaks at 1060 cm^{-1}, 1250 cm^{-1}, and 1365 cm^{-1} are severely attenuated in the sulfonated graphene oxide (GO-SO$_3$H) spectrum. The peaks at 1175 cm^{-1}, 1126 cm^{-1}, and 1040 cm^{-1} (two ν_{S-O} and one $\nu_{s-phenyl}$) confirm the presence of a sulfonic acid group, and the peaks at 1007 cm^{-1} (ν_{C-H} in-plane bending) and 830 cm^{-1} (out-of-plane hydrogen wagging) are characteristic vibrations of a *p*-disubstituted phenyl group[24]. After the final reduction with hydrazine, elemental analysis shows that there is a slight loss of sulfonic acid groups after reduction, for example, decreasing the S:C ratio from 1:41 to 1:46. The absence of the peaks at 1365 cm^{-1}, 1250 cm^{-1}, and 1060 cm^{-1} indicates the epoxide and the hydroxyl groups attached to the basal graphene layer have been removed. There is FTIR evidence of C=O (1720 cm^{-1}) even after a 48 h reaction with hydrazine. However, since the carbonyl groups are believed to come from acid moieties localized on the edge of graphene sheets[23], their presence should not deleteriously impact the electronic properties of graphene.

AFM images confirm that evaporated dispersions of graphene oxide and graphene are comprised of isolated graphitic sheets (Figure 3a,b). The graphene oxide has lateral dimensions of several micrometers and a thickness of 1 nm, which is characteristic of a fully exfoliated graphene oxide sheet.[6,13] After the final reduction step, the lateral dimensions of graphene range from several hundred nanometers to several micrometers. Undulations of graphene's surface dried on the mica substrate increases its apparent thickness (1.2 nm) measured by AFM. Graphene oxide sheets with the lateral size up to 10 μm were observed in Figure 3c; overexposure to sonication causes the defects (small holes) in the sheets. The decrease in lateral dimensions of graphene sheets is also attributed to excessive sonication during each step of the preparation of graphene. With well-controlled sonication, graphene sheets with the size comparable to those manually peeled off the top surface of small mesas of pyrolytic graphite could be obtained. Figure 3d shows a TEM image of a single graphene sheet. It appears transparent and is folded over on one edge with isolated small fragments of graphene on its surface. These observations indicate the water-soluble graphene is similar to single graphene sheets peeled from pyrolytic graphite (0.9 nm thick).[5]

The electrical conductivity is perhaps the best indicator of the extent to which graphite oxide has been reduced to graphene. A thin evaporated film ($\sim$3 μm thick) of water-soluble graphene (graphite oxide, sulfonated graphene oxide, and graphite flakes) was prepared on a glass slide. Before electrical conductivity measurements, the film is dried at 120

Table 1. Electrical Conductivity of Graphite Oxide, Sulfonated Graphene Oxide, Graphene, and Graphite

	graphite oxide	sulfonated graphene oxide	graphene	graphite
electrical conductivity (S/m)		17	1250	6120

°C to remove residual water trapped in the film. The conductivity of sulfonated graphene oxide (GO-SO$_3$H), graphene, and graphite is shown in Table 1. Graphite oxide is not conductive because it lacks an extended π-conjugated orbital system. After prereduction, the conductivity of GO-SO$_3$H product is 17 S/m, indicating a partial restoration of conjugation. Further reduction of GO-SO$_3$H to graphene with hydrazine resulted in $a > 70$-fold increase in the conductivity to 1250 S/m. By comparison, the conductivity of similarly deposited graphite flakes measured under the same conditions (6120 S/m) is only 4 times higher than that of the evaporated graphene film. The electrical conductivity of the contiguous evaporated layer of graphene implies that the extensive conjugated sp^2-carbon network is restored in the water-soluble graphene. The conductivities in Table 1 are lower bounds since the measurement has contributions from both in-plane and through-plane electron conduction combined with percolating contact resistances in the evaporated film. And moreover, the lateral dimensions of the graphite flakes ($30-40$ μm) are more than an order of magnitude larger than the dimensions of the water-soluble graphene sheets, and lateral dimensions affect the measured conductivity.

In summary, we presented a route to isolated, water-soluble graphene that is amenable to bulk production. In our product, the majority of oxygen-containing functional groups are removed. The water-soluble graphene exists in the form of single carbon sheets exhibiting an electrical conductivity comparable to graphite. With further surface modifications, graphene that is soluble in organic solvents should be accessible thereby further expediting the application of graphene in composite materials, emissive displays, micromechanical resonators, transistors, and ultrasensitive chemical detectors.[2–7]

Supporting Information Available: Descriptions of graphene synthesis, AFM, TEM, ATR-FTIR, MAS NMR, zeta potential, and electrical conductivity measurements. This material is available free of charge via the Internet at http://pubs.acs.org.

References

(1) Geim, A. K.; MacDonald, A. H. *Phys.Today* **2007**, *60*, 35–41.
(2) Ponomarenko, L. A.; Schedin, F.; Katsnelson, M. I.; Yang, R.; Hill, E. W.; Novoselov, K. S.; Geim, A. K. *Science* **2008**, *320*, 356–358.
(3) Novoselov, K. S.; Geim, A. K.; Morozov, S. V.; Jiang, D.; Zhang, Y.; Dubonos, S. V.; Grigorieva, I. V.; Firsov, A. A. *Science* **2004**, *306*, 666–669.
(4) Novoselov, K. S.; Jiang, Z.; Zhang, Y.; Morozov, S. V.; Stormer, H. L.; Zeitler, U.; Maan, J. C.; Boebinger, G. S.; Kim, P.; Geim, A. K. *Science* **2007**, *315*, 1379–1379.
(5) Geim, A. K.; Novoselov, K. S. *Nat. Mater.* **2007**, *6*, 183–191.
(6) Stankovich, S.; Dikin, D. A.; Dommmett, G. H. B.; Kohlhaas, K. M.; Zimney, E. J.; Stach, E. A.; Piner, R. D.; Nguyen, S. T.; Ruoff, R. S. *Nature* **2006**, *442*, 282–286.
(7) Watcharotone, S.; Dikin, D. A.; Stankovich, S.; Piner, R.; Jung, I.; Dommett, H. B.; Evmenenko, G.; Wu, S.-E.; Chen, S.-F.; Liu, C.-P.; Nguyen, S. T.; Ruoff, R. S. *Nano Lett.* **2007**, *7*, 1888–1892.
(8) Zacharia, R.; Ulbricht, H.; Hertel, T. *Phys. Rev. B* **2004**, *69*, 155406–155407.
(9) Gilje, S.; Han, S.; Wang, M.; Kang, K. L.; Kaner, R. B. *Nano Lett.* **2007**, *7*, 3394–3398.
(10) Gomez-Navarro, C.; Weitz, R. T.; Bittner, A. M.; Scolari, M.; Mews, A.; Burghard, M.; Kern, K. *Nano Lett.* **2007**, *7*, 3499–3503.
(11) Schniepp, H. C.; Li, J.-L.; McAllister, M. J.; Sai, H.; Herrera-Alonso, M.; Adamson, D. H.; Prud'homme, R. K.; Car, R.; Saville, D. A.; Aksay, I. A. *J. Phys. Chem. B* **2006**, *110*, 8535–8539.
(12) Niyogi, S.; Bekyarova, E.; Itkis, M. E.; McWilliams, J. L.; Hammon, M. A.; Haddon, R. C. *J. Am. Chem. Soc.* **2006**, *128*, 7720–7721.
(13) Stankovich, S.; Piner, R. D.; Chen, X.; Wu, N.; Nguyen, S. T.; Ruoff, R. S. *J. Mater. Chem.* **2006**, *16*, 155–158.
(14) Chen, J.; Hamon, M. A.; Hu, H.; Rao, A. M.; Eklund, P. C.; Haddon, R. C. *Science* **1998**, *282*, 95–98.
(15) Kunznetsova, A.; Popova, I.; Yates, J.; Bronikowski, M. J.; Huffman, C. B.; Liu, J.; Smalley, R. E.; Hwu, H. H.; Chen, J. *J. Am. Chem. Soc.* **2001**, *123*, 10699–10704.
(16) Niyogi, S.; Hammon, M. A.; Hu, H.; Zhao, B.; Bhowmik, P.; Sen, R.; Itkis, M. E.; Haddon, R. C. *Acc. Chem. Res.* **2002**, *35*, 1105–1113.
(17) Zhang, J.; Zou, H.; Qing, Q.; Yang, Y.; Li, Q.; Liu, Z.; Guo, X.; Du, Z. *J. Phys. Chem. B* **2003**, *107*, 3712–3718.
(18) Li, D.; Muller, M. B.; Gilje, S.; Kaner, R. B.; Wallace, G. G. *Nat. Nano.* **2008**, *3*, 101–105.
(19) Hummer, W.; Offeman, R. *J. Am. Chem. Soc.* **1958**, *80*, 1339–1340.
(20) Hontoria-Lucas, C.; Lopez-Peinado, A. J.; Lopez-Gonzalez, J. D. D.; Rojas-Cervantes, M. L.; Martin-Aranda, R. M. *Carbon* **1995**, *33*, 1585–1592.
(21) *Zeta Potential of Colloids in Water and Waste Water*, ASTM Standard D 4187–82, American Society for Testing and Materials, 1985.
(22) Titelman, G. I.; Gelman, V.; Bron, S.; Khalfin, R. L.; Cohen, Y.; Bianco-Peled, H. *Carbon* **2005**, *43*, 641–649.
(23) Stankovich, S.; Dikin, D. A.; Piner, R. D.; Kohlhaas, K. A.; Kleinhammes, A.; Jia, Y.; Wu, Y.; Nguyen, S. T.; Ruoff, R. S. *Carbon* **2007**, *45*, 1558–1565.
(24) Colthup, N. B.; Daly, L. H.; Wiberley, S. E. *Introduction to Infrared and Raman Spectroscopy*, 3rd ed.; Academic Press: London, 1990.
(25) Stankovich, S.; Piner, R. D.; Nguyen, S. T.; Ruoff, R. S. *Carbon* **2006**, *44*, 3342–3347.

NL080604H